Optical Properties of CdS Nanocrystals Doped with Zinc and Copper

Article *in* Semiconductors · October 2018

DOI: 10.1134/S1063782619030138

CITATION
1

READS
132

5 authors, including:

Yu. A. Nitsuk
Odessa National University
24 PUBLICATIONS **88** CITATIONS
SEE PROFILE

Maria I Kiose
Moscow State Linguistic University
10 PUBLICATIONS **6** CITATIONS
SEE PROFILE

Yu. F. Vaksman
Odessa National University
34 PUBLICATIONS **116** CITATIONS
SEE PROFILE

V. Smyntyna
Odessa National University
309 PUBLICATIONS **1,246** CITATIONS
SEE PROFILE

ISSN 1063-7826, Semiconductors, 2019, Vol. 53, No. 3, pp. 361–367. © Pleiades Publishing, Ltd., 2019.
Russian Text © Yu.A. Nitsuk, M.I. Kiose, Yu.F. Vaksman, V.A. Smyntyna, I.R. Yatsunskyi, 2019, published in Fizika i Tekhnika Poluprovodnikov, 2019, Vol. 53, No. 3, pp. 381–387.

MICROCRYSTALLINE, NANOCRYSTALLINE, POROUS, AND COMPOSITE SEMICONDUCTORS

Optical Properties of CdS Nanocrystals Doped with Zinc and Copper

Yu. A. Nitsuk[a,*], M. I. Kiose[a], Yu. F. Vaksman[a], V. A. Smyntyna[a], and I. R. Yatsunskyi[b]

[a] *Mechnikov National University, Odessa, 65082 Ukraine*
[b] *Adam Mickiewicz University, Poznan, 61-712 Poland*
**e-mail: nitsuk@onu.edu.ua*

Received September 17, 2018; accepted October 9, 2018

Abstract—Cadmium-sulfide nanocrystals are produced by the colloidal method. Doping with zinc and copper is conducted during nanocrystal growth. The optical absorption and photoluminescence spectra are studied. The maximum concentration of the optically active copper impurity is determined from a shift of the fundamental absorption edge to lower energies. It is shown that the long-wavelength luminescence of CdS and CdS:Zn nanocrystals is defined by optical transitions at donor–acceptor pairs. In CdS:Cu nanocrystals, optical absorption and photoluminescence in the visible spectral region are defined by recombination transitions involving the ground state of Cu_{Zn}^{2+} ions. The infrared absorption and photoluminescence of CdS:Cu quantum dots are defined by intracenter transitions within Cu_{Zn}^{2+} ions.

DOI: 10.1134/S1063782619030138

1. INTRODUCTION

Semiconductor nanocrystals of the II–VI group are finding more and more applications in present-day electronics. Currently available technologies of synthesis make it possible to produce nanocrystals with a narrow size distribution, a specified surface morphology, and a high degree of stability. The possibility of controlling the band gap and of tuning the luminescence wavelength makes such materials promising for use in optoelectronics. Luminescing semiconductor nanoparticles that exhibit a wide absorption spectrum and well-pronounced narrow luminescence peaks in the visible and near-infrared (IR) spectral regions offer considerable promise for medical diagnostics [1].

In the series of II–VI semiconductor nanocrystals, cadmium-sulfide nanocrystals are studied most extensively. The advantages of this material are its low-price and simple methods of production and a high quantum efficiency of emission in the visible spectral region [2]. Numerous studies of the luminescence properties of CdS nanocrystals have shown that broad multicomponent emission bands observed in the range 450–800 nm are dominant in the emission spectra [3, 4]. Changes in the nanoparticle dimensions under variations in different technological parameters (the content of precursors and stabilizers of growth, the pH indicator and temperature of the medium, etc.) bring about the redistribution of intensities of elementary emission lines only, whereas their spectral positions remain unchanged.

The purpose of this study is to search for a method of controlling the spectral position of long-wavelength emission bands of CdS nanocrystals by doping with zinc and copper impurities and to establish the nature of optical and luminescence transitions in undoped CdS and doped CdS:Zn and CdS:Cu nanocrystals.

2. EXPERIMENTAL

We here studied CdS nanocrystals chemically produced for commercial reagents (Beijing Reagent Company). As the sources of cadmium ions and sulfur ions, we used cadmium chloride and sodium sulfide, respectively. To dope with copper or zinc, a 10% solution of zinc chloride or copper chloride was added to a 10% solution of cadmium chloride. The reactions of the synthesis of nanoparticles were conducted in a 5% solution of gelatin and could be described as:

$$CdCl_2 + Na_2S \rightarrow CdS\downarrow + NaCl, \quad (1)$$

$$CdCl_2 + ZnCl_2 + Na_2S \rightarrow CdS:Zn\downarrow + 2NaCl + Cl_2\uparrow, \quad (2)$$

$$CdCl_2 + CuCl_2 + Na_2S \rightarrow CdS:Cu\downarrow + 2NaCl + Cl_2\uparrow. \quad (3)$$

After removal of the reaction products that were not required, the colloidal solution of nanoparticles was applied over a quartz substrate and placed into a thermostat until the polymer film dried. For X-ray diffraction (XRD) and scanning electron microscopy (SEM) studies, the solution was applied over silicon substrates. It is found that, in the XRD patterns, the peaks corresponding to the (100), (002), (102), (110),

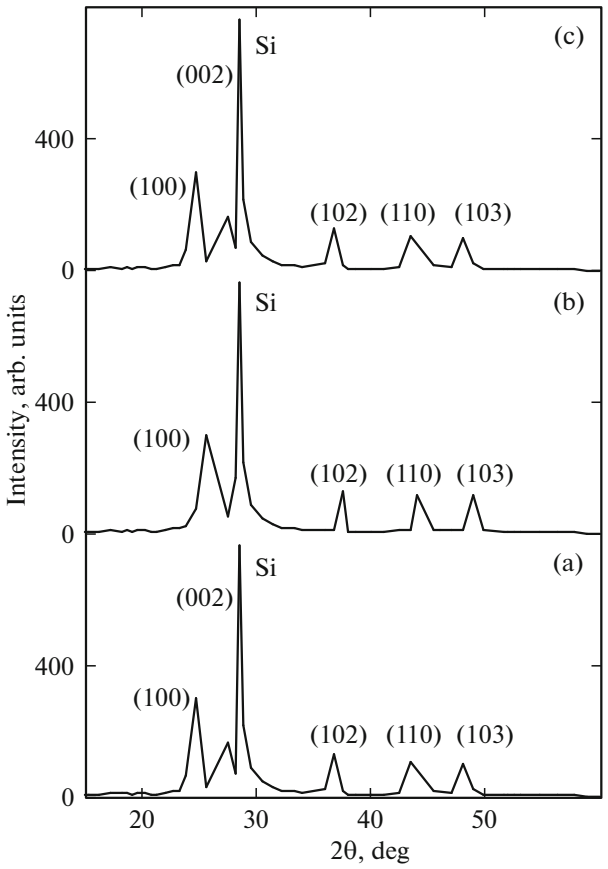

Fig. 1. XRD patterns of (a) CdS, (b) Cds:Zn, and (c) CdS:Cu nanocrystals.

and (103) planes in CdS are dominant (Fig. 1a). Similar planes were detected in CdS:Zn (Fig. 1b) and CdS:Cu (Fig. 1c) crystals.

To establish the nature of optical and luminescence transitions in the nanocrystals under study and to determine the average nanoparticle dimensions and the concentration of optically active impurities, we studied the optical density and photoluminescence (PL) spectra. To do this, we chose a series of samples produced from different amounts of the initial and impurity components (see Table 1).

The optical density spectra were recorded using an MDR-6 monochromator with 1200 and 600 bar mm^{-1} gratings for studies in the visible and IR spectral regions, respectively. As the detector of radiation in the visible spectral region, we used an FEU-100 photoelectron multiplier. The IR emission signal was detected with an FR-1P IR photoresistor operating in the ac mode of detection.

The visible PL spectra were recorded with an ISP-51 prismatic spectrograph. Emission was recorded with the FEU-100 photoelectron multiplier. The IR PL signal was studied with the MDR-6 monochromator and recorded with the IR photoresist. The luminescence signal was excited using light-emitting diodes (Edison Opto Corporation), with maxima of emission at 375, 400, 460, 550, and 640 nm, and an ILGI-503 pulsed nitrogen laser emitting at a wavelength of 331.7 nm. The optical density and PL were studied at room temperature.

To clarify the nature of centers responsible for the luminescence and optical properties of CdS:Cu nanocrystals, measurements were carried out in the temperature range 293–423 K. During the measurements, the temperature in this range was kept constant with the use of a cryostat.

3. OPTICAL DENSITY STUDIES

The optical density spectra of undoped CdS nanocrystals are shown in Fig. 2. It is established that a decrease in the initial content of cadmium chloride and sodium sulfide from 0.1 to 0.01% yields a shift of the band-gap edge to higher energies, from 2.46 to 3.12 eV. This result is supported by a change in the color of the colloidal solutions from orange to colorless.

From an increase in the band gap (ΔE_g) compared to the band gap of the bulk crystal, we estimated the

Table 1. Optical characteristics of CdS, CdS:Zn, and CdS:Cu nanocrystals in the region of the absorption edge

Sample number	Nanocrystal type	E_g, eV	ΔE_g, meV	R, nm
1	CdS, 0.01%$CdCl_2$, 0.01%Na_2S	3.12	0.72	4.8
2	CdS, 0.02%$CdCl_2$, 0.02%Na_2S	3.02	0.62	5.3
3	CdS, 0.03%$CdCl_2$, 0.03%Na_2S	2.95	0.55	5.8
4	CdS, 0.1%$CdCl_2$, 0.1%Na_2S	2.46	0.06	17.0
5	CdS : Zn, 0.02$CdCl_2$ + 0.01%$ZnCl_2$, 0.02%Na_2S	3.19	0.79	4.7
6	CdS : Zn, 0.02$ZnCl_2$ + 0.02%$CdCl_2$, 0.02%Na_2S	3.3	0.9	4.4
7	CdS : Cu, 0.02%$ZnCl_2$ + 0.001%$CuCl_2$, 0.02%Na_2S	2.89	0.49	6.0
8	CdS : Cu, 0.02%$ZnCl_2$ + 0.005%$CuCl_2$, 0.02%Na_2S	2.73	0.33	7.3
9	CdS : Cu, 0.02%$ZnCl_2$ + 0.01%$CuCl_2$, 0.02%Na_2S	2.68	0.28	8.0

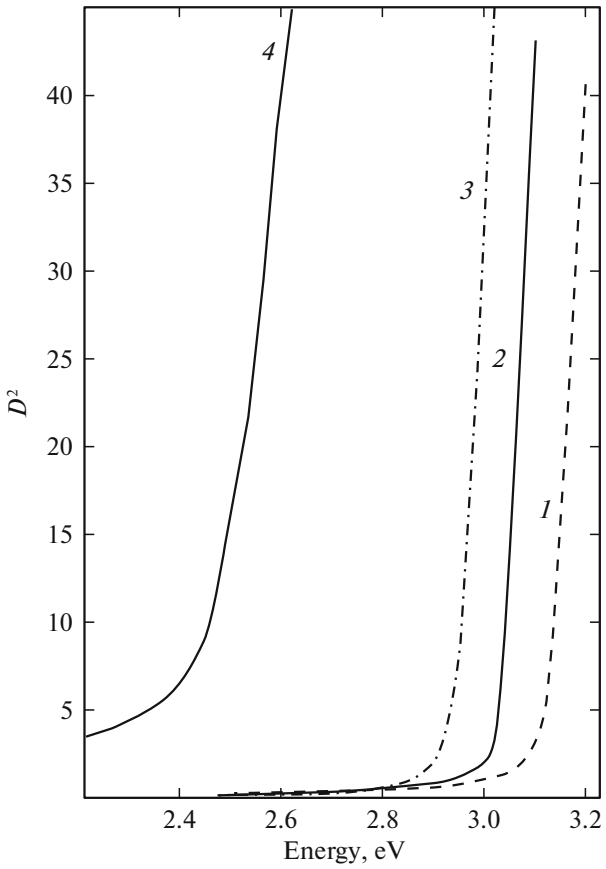

Fig. 2. Optical density spectra of CdS nanocrystals for samples (*1*) 1, (*2*) 2, (*3*) 3, and (*4*) 4.

average nanoparticle radius R in the effective-mass approximation, using the formula from [5]:

$$R = \frac{h}{\sqrt{8\mu\Delta E_g}}. \quad (4)$$

Here, h is Planck's constant, $\mu = ((m_e^*)^{-1} + (m_h^*)^{-1})^{-1}$, where $m_e^* = 0.19m_e$ and $m_h^* = 0.8m_e$ are, correspondingly, the electron and hole effective masses in cadmium sulfide, m_e is the free electron mass, and ΔE_g is the difference between the band gaps in the CdS nanoparticle and bulk crystal (2.4 eV). The results of the calculations are given in Table 1. The results obtained here are supported by the SEM studies. The SEM images of sample 2 are shown in Fig. 3. In Fig. 3, we can see the formation of nanoparticles 3–6 nm in dimensions.

Upon doping with zinc, the absorption edge shifts to higher energies (Fig. 4). In this case, the shift increases, as the content of zinc is increased. A similar blue shift was observed previously [6]. The increase in the band gap upon doping with zinc can be interpreted as a result of formation of the $Cd_xZn_{1-x}S$ ternary compound. In [6], this effect is related to an increase in the lattice period. In the XRD patterns of heavily doped

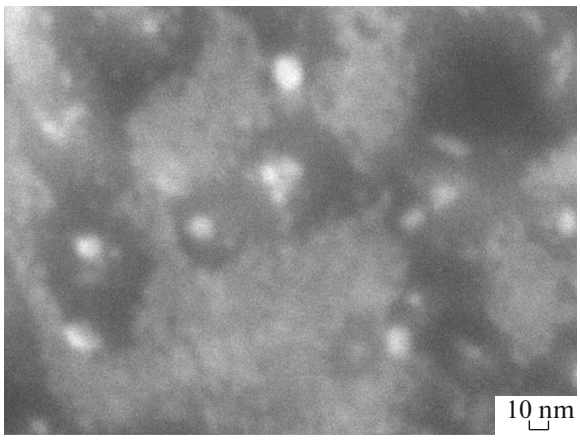

Fig. 3. SEM image of CdS nanocrystals (sample 2).

CdS:Zn nanocrystals (Fig. 1b), we observe a shift of the diffraction peaks to larger angles.

In the range 2.4–1.4 eV of the optical density spectra of CdS and CdS:Zn nanocrystals, no features are detected.

In nanocrystals doped with copper, we observe a shift of the absorption edge to lower energies, as the content of $CuCl_2$ is increased (Fig. 5). This shift can be attributed to an increase in the nanoparticle size and to interimpurity Coulomb interaction that is characteristic of transition-element impurities [7–11]. Using the relation from [12]

$$\Delta E_g = 2\times10^5\left(\frac{3}{\pi}\right)^{1/3}\frac{eN^{1/3}}{4\pi\varepsilon_0\varepsilon_s}, \quad (5)$$

where e is the elementary charge, N is the concentration of copper impurities (in cm^{-3}) and $\varepsilon_s = 8.9$ is the static permittivity of cadmium sulfide. From the value of the shift between the band gaps of CdS:Cu nanoparticles (sample 2) and undoped CdS nanocrystals (samples 7, 8, 9, see Table 1), we calculated the copper concentration in the CdS:Cu nanocrystals under study. The maximum concentration of optically active copper is 10^{21} cm^{-3} in nanocrystals containing 0.01% of $CuCl_2$. As the content of $CuCl_2$ is lowered to 0.005 and 0.001%, the concentration of optically active Cu impurities decreases, correspondingly, to 8×10^{20} and 6×10^{19} cm^{-3}. The high concentrations of optically active Cu impurities are indicative of the efficient incorporation of Cu atoms into the Cd sublattice upon doping by the method used in the study.

In addition, it is known that the doping of semiconductor compounds with transition-element impurities brings about the appearance of absorption lines in the visible and IR spectral regions. In the CdS:Cu nanocrystals under study, we observe an impurity absorption band in the visible region (see inset in Fig. 5). An increase in the concentration of copper impurities yields an increase in absorption in this

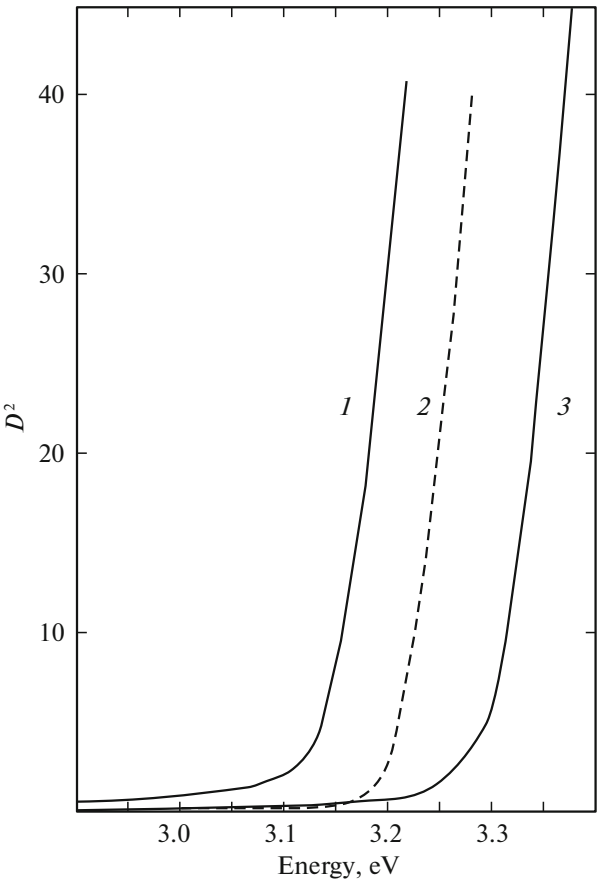

Fig. 4. Optical density spectra of (*1*) CdS and (*2*, *3*) CdS:Zn nanocrystals for samples (*1*) 1, (*2*) 5, (*3*) 6.

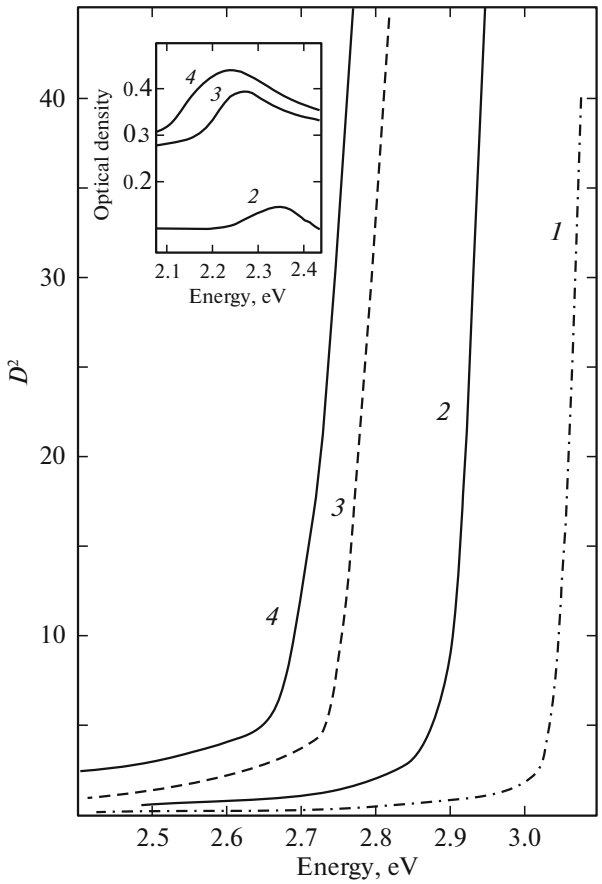

Fig. 5. Optical density spectra of (*1*) CdS and (*2–4*) CdS:Cu nanocrystals for samples (*1*) 3, (*2*) 7, (*3*) 8, and (*4*) 9. Inset: optical density spectra of CdS:Cu nanocrystals in the visible region.

region, and the absorption maximum shifts to lower energies, from 2.49 to 2.28 eV. The shift correlates with the changes in the band gap of CdSe:Cu nanocrystals. As the temperature of the nanocrystals is elevated from 293 to 423 K, the absorption band is shifted to lower energies by 0.05 eV. This shift corresponds to the temperature change in the band gap of CdS. Such behavior is typical of absorption lines defined by impurity-level–band optical transitions. From the difference between the band gap of CdS:Cu nanocrystals and the position of the maximum of the absorption line, we determined the depth of the copper impurity level with respect to the top of the valence band. This depth is found to be 0.4 eV. From comparison with the case of bulk crystals, we can conceive that such a depth corresponds to the ground state $^2T_2(D)$ of Cu^{2+}_{Zn} ions.

The absorption spectra in the IR region exhibit lines at the energies 0.86, 1.12, and 1.32 eV (Fig. 6, curves *1–3*). As the concentration of dopants is increased, the absorption increases, whereas the positions of these lines remain unchanged. The positions of these lines remain unchanged under variations in the temperature of the samples under study as well. Such behavior is characteristic of intracenter absorption lines. For Cu^{2+} ions in bulk crystals, the only intracenter absorption line is caused by $^2T_2(D) \rightarrow {}^2E_2(D)$ transitions [13].

According to the data of [14], the three absorption lines observed in the nanocrystals under study can be interpreted as a result of trigonal distortion of the crystal field and the effect of this distortion on the strength of the crystal field D_q.

Another cause of the appearance of the three absorption lines can be the effect of the crystallite dimensions on the strength of the crystal field D_q [15].

We suppose that the existence of the triplet can be attributed to the reaction-induced formation of CdS:Cu nanoparticles, in which the Cu^{2+} ions are surrounded by different ligands (tetrahedral, octahedral, or trigonal surroundings). According to the data of [16], the smallest splitting occurs in the tetrahedral surroundings. In the case under consideration, the line at the minimum energy well coincides with the absorption lines of tetrahedrally coordinated Cu^{2+} ions in CdS bulk crystals. The lines observed at higher energies correspond to the octahedral and trigonal

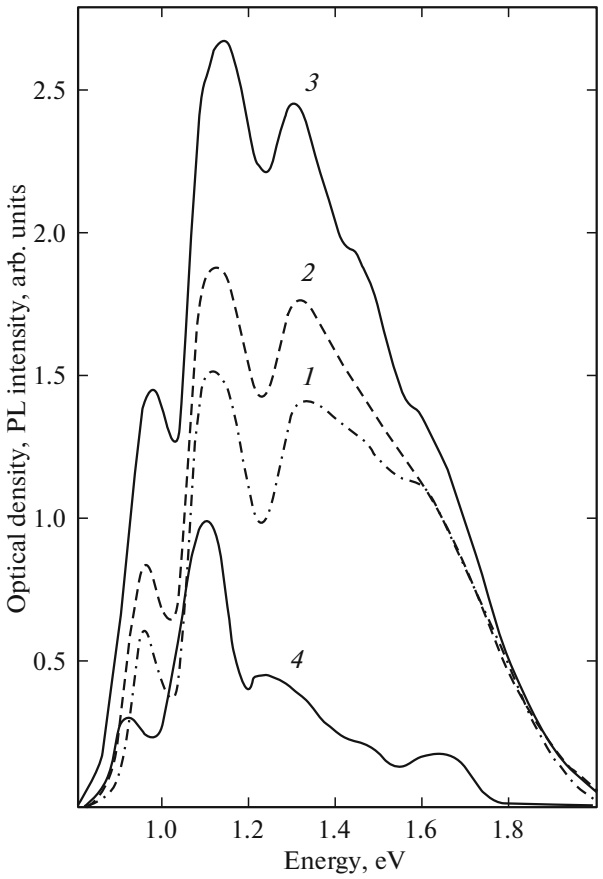

Fig. 6. (*1*–*3*) Optical density and (*4*) PL spectra of CdS:Cu nanocrystals in the IR region for samples (*1*) 7, (*2*, *4*) 8, and (*3*) 9.

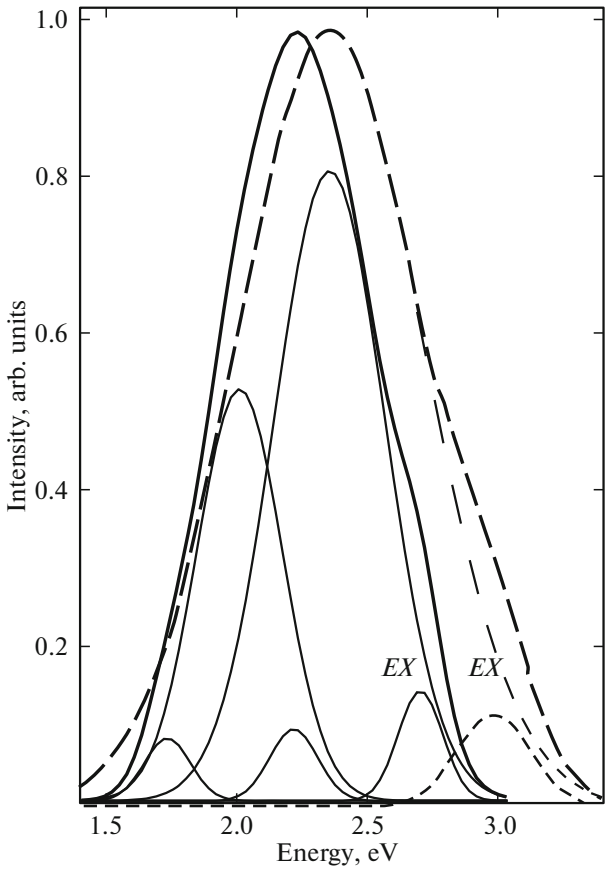

Fig. 7. PL spectra of (solid lines) CdS (sample 3) and (dashed lines) CdS:Zn (sample 6) nanocrystals.

surroundings. In this case, the trigonal surrounding experiences considerable distortions, which manifest themselves in the presence of slightly resolved absorption lines in the range 1.4–1.6 eV. Support for this hypothesis is provided by the observation of diffraction peaks corresponding to different crystal planes (Fig. 1).

4. PL STUDIES

Undoped CdS nanocrystals at room temperature exhibit broad multicomponent visible emission bands in the range 1.6–2.8 eV (Fig. 7). For crystals with a low content of precursors (0.01–0.03%), decomposition of the bands into elementary Gaussian components reveals six elementary emission lines at 1.6, 1.8, 2.0, 2.13, 2.36, and 2.6 eV (Fig. 7). The high-energy emission line shifts to higher energies, as the content of the precursors is lowered. We establish a correlation of the position of this line with the band gap. This allows us to assume that these emission lines are of excitonic nature. The large shift (0.2 eV) allows us to assume that there exist excitons bound at point defects. From the conditions of synthesis at a low content of cadmium precursors, we can conceive that such defects can be cadmium vacancies that serve as acceptors.

The positions of the other five emission lines are independent of a variation in the band gap of the nanocrystals and coincide with the positions of previously studied emission lines at donor–acceptor pairs in CdS bulk crystals. The 1.6- and 1.8-eV emission lines are caused by transitions involving $(V_S^+, V_{Cd}^{2-})^-$ pairs with different spacings between them [17]. The 2.02- and 2.12-eV emission lines are attributed to $(Cd_i^+, V_{Cd}^{2-})^-$ centers with different spacings between the pairs [18]. The 2.36-eV emission line is attributed to neutral $(V_S^+, V_{Cd^-})^*$ vacancies [19].

As the content of the precursors is increased, the fraction of interstitial cadmium atoms Cd_i^+ in the nanocrystals increases. This inference is supported by the fact that, in such samples, there are only 2.02- and 2.12-eV emission lines.

In CdS:Zn crystals, the structure and spectrum of the five emission lines at donor–acceptor pairs is retained. The 2.36-eV emission line is dominant, and the exciton-emission line shifts, together with the absorption edge, to higher energies (Fig. 7). A similar

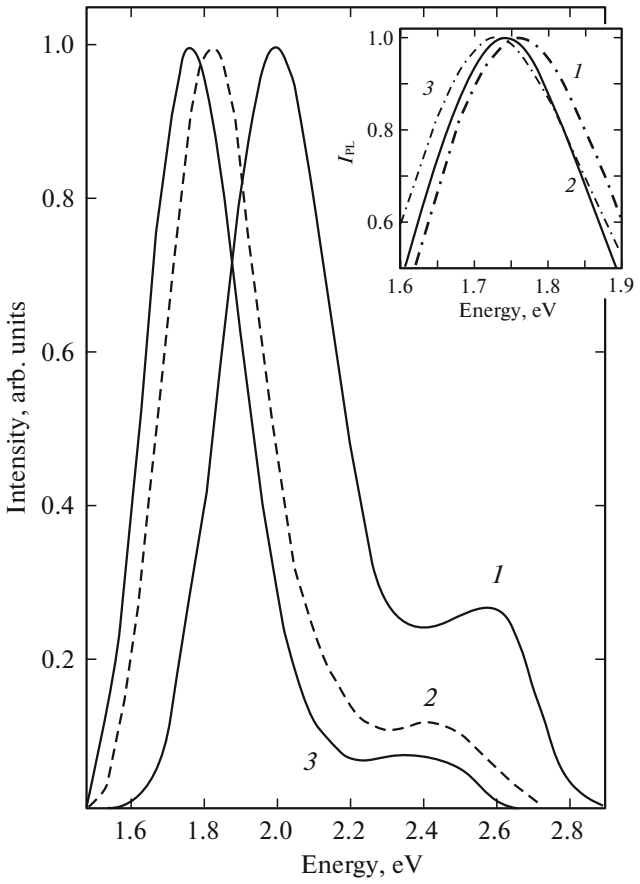

Fig. 8. PL spectra of CdS:Cu nanocrystals for samples (*1*) 7, (*2*) 8, and (*3*) 9. Inset: PL spectra recorded for sample 9 at (*1*) 293, (*2*) 353, and (*3*) 423 K.

shift of the exciton-emission lines was observed previously [6].

Doping with copper during the growth of nanocrystals brings about the quenching of emission lines at donor–acceptor pairs, and the exciton-emission line shifts to lower energies with respect to the exciton lines in undoped CdS nanocrystals (Fig. 8). It is found that the intensity of this line decreases, as the content of copper is increased. This can be attributed to the substitution of copper atoms for cadmium vacancies during synthesis.

In the long-wavelength region of the spectrum of CdS:Cu nanocrystals, we observe an emission band, whose intensity increases, as the content of copper is increased. The emission maximum shifts from 2 eV at a content of copper 0.001% to 1.78 eV at a content of 0.01% (Fig. 8). This shift coincides with a change in concentration in the band gap and with a concentration shift of the absorption band in the visible spectral region (Fig. 5) in CdS:Cu nanocrystals. The temperature shift of these emission lines from the visible spectral region to the near-IR region upon heating from 293 to 423 K (see inset in Fig. 8) corresponds to the temperature change in the band gap of CdS. The maximum emission intensity is observed upon excitation at the photon energies 2.6 and 2.25 eV that fall into the impurity absorption bands in these nanocrystals. This allows us to assume that the centers responsible for absorption and luminescence are identical in nature. According to the data of [20], emission in this region is caused by transitions of electrons from the conduction band to the ground state $^2T_2(D)$ of Cu_{Zn}^{2+} ions. The Stokes shift is 0.5 eV in all of the samples.

In the mid-IR region of the spectrum of CdS:Cu nanocrystals excited at the photon energy E_{ex} = 2.25 eV, we observe a series of three emission lines at 0.92, 1.1, and 1.24 eV (Fig. 6, curve *4*). As the sample temperature and the content of the impurities are increased, the positions of these lines remain unchanged, whereas the intensities increase, as the content of $CuCl_2$ is increased to 0.03%. Such behavior is characteristic of intracenter emission lines. These emission lines correlate with the previously studied absorption lines (Fig. 6, curves *1*–*3*). The Stokes shift is 30–60 meV.

It should be noted that, as the content of $CuCl_2$ is increased to 0.05%, we observe concentration quenching of the PL signal in the near- and mid-IR regions.

5. CONCLUSIONS

The results of the above-described studies make it possible to draw the following conclusions:

(i) By varying the content of precursors, it is possible to influence the nanoparticle size in the CdS nanocrystals and their long-wavelength self-activated luminescence spectrum.

(ii) The addition of the zinc impurity brings about a shift of the exciton luminescence of CdS to higher energies. In self-activated emission, the green band with a maximum at 2.36 eV becomes dominant.

(iii) Doping with copper results in a shift of the fundamental absorption edge and exciton-emission lines of CdS to lower energies. From the shift, the maximum concentration of optically active copper impurities in CdS nanocrystals is determined. This concentration is found to be in the range from 6×10^{19} cm^{-3} for CdS nanocrystals containing 0.001% of $CuCl_2$ to 10^{21} cm^{-3} in CdS nanocrystals containing 0.01% of $CuCl_2$.

(iv) The visible emission of CdS:Cu nanocrystals is represented by an impurity emission band defined by radiative transitions from the conduction band to the ground state $^2T_2(D)$ of Cu_{Zn}^{2+} ions.

(v) The IR absorption and PL of CdS:Cu nanocrystals are caused by intracenter optical transitions within Cu_{Zn}^{2+} ions surrounded by different types of environments.

REFERENCES

1. S. V. Rempel', A. D. Levin, A. Yu. Sadagov, and A. A. Rempel', Phys. Solid State **57**, 1103 (2015).
2. V. I. Kochubey, D. I. Kochubey, Yu. G. Konyukhova, I. V. Zabenkov, S. I. Tatarinov, and E. K. Volkova, Opt. Spectrosc. **109**, 154 (2010).
3. V. G. Klyuev, Fam Tkhi Khan M'en, and Yu. S. Bezdetko, Kondens. Sredy Mezhfaz. Granitsy **16** (1), 27 (2014).
4. V. Smyntyna, B. Semenenko, V. Skobeeva, and N. Malushin, Beilstein J. Nanotechnol. **5**, 355 (2014).
5. A. I. Gusev and A. A. Rempel', *Nanocrystalline Materials* (Fizmatlit, Moscow, 2000; Cambridge Int. Sci., Cambridge, 2004), p. 224.
6. D. V. Korbutyak, S. V. Tokarev, S. I. Budzulyak, A. O. Kuryk, V. P. Kladko, Yu. O. Polishchuk, O. M. Shevchuk, H. A. Ilshuk, and V. S. Tokarev, Phys. Chem. Solid State **14**, 222 (2013).
7. Yu. F. Vaksman, V. V. Pavlov, Yu. A. Nitsuk, Yu. N. Purtov, A. S. Nasibov, and P. V. Shapkin, Semiconductors **39**, 377 (2005).
8. Yu. F. Vaksman, Yu. A. Nitsuk, V. V. Yatsun, A. S. Nasibov, and P. V. Shapkin, Semiconductors **44**, 444 (2010).
9. Yu. F. Vaksman, V. V. Pavlov, Yu. A. Nitsuk, Yu. N. Purtov, A. S. Nasibov, and P. V. Shapkin, Funct. Mater. **14**, 426 (2007).
10. Yu. A. Nitsuk, Semiconductors **48**, 142 (2014).
11. I. Radevici, N. Nedeoglo, K. Sushkevich, D. Nedeoglo, H. Huhtinen, and P. Paturi, Phys. B (Amsterdam, Neth.) **503**, 11 (2016).
12. Yu. F. Vaksman, Yu. A. Nitsuk, Yu. N. Purtov, and P. V. Shapkin, Semiconductors **35**, 883 (2001).
13. T. Telahun, U. Scherz, P. Thurian, R. Heitz, A. Hoffmann, and I. Broser, Phys. Rev. B **53**, 1274 (1996).
14. S. Y. Wu, H. M. Zhang, H. N. Dong, X. F. Wang, and Y. X. Hu, Phys. Chem. Minerals **36**, 483 (2009).
15. R. Shimkiv, S. Sveleba, I. Karpa, I. Katerinchuk, I. Kun'o, and O. Fitsich, in *Proceedings of the Conference on Semiconductor Physics Lashkarev' Readings, Kiev, Ukraina, 2011,* p. 59.
16. J. N. Murrell, S. F.-A. Kettle, and J. M. Tedder, *The Chemical Bond* (Wiley, Chichester, 1978), p. 249.
17. I. B. Ermolovich, G. I. Matvievskaya, G. S. Pekar', and M. K. Sheinkman, Ukr. Fiz. Zh. **18**, 732 (1973).
18. V. V. Gorbunov, S. S. Ostapenko, M. A. Tanatar, and M. K. Sheinkman, Sov. Phys. Solid State **23**, 1928 (1981).
19. I. B. Ermolovich, G. I. Matvievskaya, and M. K. Sheikman, Sov. Phys. Semicond. **9**, 1070 (1975).
20. V. E. Lashkarev, M. K. Sheinkman, and I. B. Ermolovic, in *Proceedings of the International Conference on II–VI Compounds, New York, 1967,* p. 711.

Translated by E. Smorgonskaya